

---

# HyperFlexis: Joint Design of Algorithms and Systems for Multi-SLO Serving and Fast Scaling

Zahra Yousefijamarani<sup>1,3,\*</sup>, Xinglu Wang<sup>1,3,\*</sup>, Qian Wang<sup>1,\*</sup>, Morgan Lindsay Heisler<sup>1</sup>, Taha Shabani<sup>1</sup>, Niloofar Gholipour<sup>1,4</sup>, Parham Yassini<sup>1</sup>, Hong Chang<sup>1</sup>, Kan Chen<sup>2</sup>, Qiantao Zhang<sup>2</sup>, Xiaolong Bai<sup>2</sup>, Jiannan Wang<sup>3</sup>, Ying Xiong<sup>1</sup>, Yong Zhang<sup>1,†</sup>, Zhenan Fan<sup>1,†</sup>

<sup>1</sup>Huawei Technologies Canada Co., Ltd. , <sup>2</sup>Huawei Technologies Co., Ltd. , <sup>3</sup>Simon Fraser University ,  
<sup>4</sup>École de technologie supérieure

Modern large language model (LLM) serving systems face challenges from highly variable requests with diverse lengths, priorities, and stage-specific service-level objectives (SLOs). Meeting these requires real-time scheduling, rapid and cost-effective scaling, and support for both collocated and disaggregated Prefill/Decode (P/D) architectures.

We present **HyperFlexis**, a unified LLM serving system that integrates algorithmic and system-level innovations to jointly optimize scheduling and scaling under multiple SLOs. It features a multi-SLO-aware scheduler that leverages budget estimation and request prioritization to ensure proactive SLO compliance for both new and ongoing requests. The system supports prefill- and decode-stage multi-SLO scheduling for P/D-disaggregated architectures and KV cache transfers. It also enables cost-effective scaling decisions, prefill–decode instance linking during scaling, and rapid P/D role transitions. To accelerate scaling and reduce cold-start latency, a device-to-device (D2D) weight transfer mechanism is proposed that lowers weight loading overhead by up to **19.39**×. These optimizations allow the system to achieve up to **4.44**× higher SLO attainment, **65.82%** lower request latency, and cost parity with state-of-the-art baselines. The code will be released soon.

*Keywords:* *LLM Inference Serving, Multi-SLO Scheduling, Dynamic resource scaling, P/D disaggregated systems, P/D Compatible Scheduling*

---

<sup>\*</sup>Equal contribution.

<sup>†</sup>Corresponding authors: Yong Zhang <yong.zhang3@huawei.com>, Zhenan Fan <zhenan.fan1@huawei.com>.

# Contents

<b>1</b>	<b>Introduction</b>	<b>4</b>
<b>2</b>	<b>Background</b>	<b>5</b>
2.1	Large Language Model & LLM Service . . . . .	5
2.2	Execution Modes: Collocated vs. Disaggregated . . . . .	6
2.3	Ascend NPU . . . . .	6
2.4	Multi-SLOs Serving . . . . .	6
<b>3</b>	<b>Problem Formulation</b>	<b>6</b>
<b>4</b>	<b>HyperFlexis Overall System Design and Framework</b>	<b>8</b>
<b>5</b>	<b>Dispatching Mechanism and Policy</b>	<b>9</b>
5.1	SLO-Aware Dispatching Mechanism. . . . .	9
5.2	Priority-Based SLO Mapping . . . . .	12
<b>6</b>	<b>Scaling Mechanism and Policy</b>	<b>12</b>
<b>7</b>	<b>Experimental Setup</b>	<b>13</b>
7.1	Environment . . . . .	14
7.2	Serving Models . . . . .	14
7.3	Benchmark Workloads and Datasets . . . . .	14
7.4	Baselines . . . . .	15
7.5	Metrics . . . . .	15
<b>8</b>	<b>Evaluation</b>	<b>16</b>
8.1	Multi-task Performance Evaluation . . . . .	16
8.1.1	Collocated Architecture Results . . . . .	16
8.1.2	P/D Disaggregated Architecture Results . . . . .	17
8.2	Priority Mapping Results . . . . .	17
8.3	Fast Scaling Evaluation . . . . .	18
<b>9</b>	<b>Ablation Study</b>	<b>18</b>
9.1	Impact of Dynamic SLO Assignment . . . . .	18
9.2	Single-task Performance Evaluation . . . . .	19
9.3	Monitor and Scaling Interval . . . . .	20
<b>10</b>	<b>Related Works</b>	<b>21</b>
10.1	LLM Inference and Prompt/Decode Separation . . . . .	21
10.2	Distributed Multi-SLO Inference Systems . . . . .	22

10.3 Multi-SLO Scheduling, Placement, and Scaling . . . . .	23
<b>11 Conclusion</b>	<b>23</b>
<b>A Latency Prediction</b>	<b>30</b>
<b>B Computing Token Limit (ntoken)</b>	<b>30</b>

## 1. Introduction

The widespread adoption of large language models (LLMs) [1, 14, 28, 41, 42, 50] across diverse applications [1, 6, 20, 43, 48], has created an urgent demand for highly scalable and efficient serving systems [22]. However, serving LLMs effectively remains challenging due to strict latency requirements, high query concurrency, and limited computational resources.

A fundamental challenge is the need to satisfy diverse and often conflicting service level objectives (SLOs) associated with different types of tasks. These SLOs may range from tight latency constraints for real-time interactions to high-throughput requirements for batch jobs, and cost-efficiency demands for long-running or low-priority tasks. For example, in interactive chatbots [1], users expect fast responses with minimal latency. In contrast, large-scale document summarization tasks [48] can tolerate longer startup times but require fast token generation once the process begins. In practice, the inference cluster must handle a heterogeneous mix of such requests concurrently, requiring careful balancing of resource allocation between latency-sensitive and latency-tolerant jobs.

This variability of workloads, particularly in multi-SLO scenarios with diverse latency and throughput targets, motivates the need for elastic scalability in LLM serving systems. Rapid, fine-grained scaling is essential, as fluctuating workload intensity and request characteristics can cause one class of requests to impact others if resources cannot adapt promptly. Achieving this is non-trivial due to the complexity of resource allocation and adaptation. Collocated and disaggregated Prefill/Decode (P/D) deployments provide different strategies to handle these challenges: collocated P/D is simpler and lower-overhead, making it suitable for small-scale systems where tight coordination between prefill and decode is feasible. In contrast, disaggregated P/D [17, 57] allows the two phases to scale independently and specialize resources according to their distinct computational demands, which is crucial for large-scale deployments with heterogeneous workloads.

Another challenge for P/D disaggregated scenario is that existing systems often make a one-shot dispatching decision [59], assigning both the prefill and decode instances as soon as the request arrives. This approach has two drawbacks: first, it is difficult to accurately predict when the prefill stage will finish due to queuing delays; second, even if the prefill completion time could be estimated, the decode-stage workload distribution at that future moment is hard to foresee, potentially leading to SLO violations.

Beyond these limitations, multi-SLO workloads introduce an additional challenge: they must be scheduled across multiple servers and instances where resource contention can shift rapidly. Effectively addressing these challenges requires a system that can dynamically schedule multi-SLO requests while adaptively scaling resources across both collocated and disaggregated P/D deployments, ensuring SLO attainment under varying workloads.

Recent works have begun to explore the challenges of multi-SLO scheduling in this context. They primarily focused on single-task [13, 30, 47, 59] or single-instance [40, 52] scheduling, while some approaches address scaling [16, 38]. Although promising, these methods do not fully support multi-task, multi-instance workloads, limiting performance and efficiency.

To address the challenges of multi-SLO scheduling and elastic scaling in modern LLM serving, we introduce HyperFlexis, a unified system that combines algorithmic and system-level

innovations. Our design supports both prefill-decode disaggregated and co-located execution models.

Our system makes the following contributions:

- We propose *HyperFlexis*, a multi-SLO-aware LLM serving system that integrates scheduling and scaling to achieve high SLO compliance, low latency, and cost-efficient operation.
- We design a *Multi-SLO-Aware Dispatcher* that efficiently serves requests with heterogeneous SLOs by organizing them into SLO-aware queues and assigning them to workers via an Instance-Priority Queue. For P/D disaggregated deployments, the dispatcher schedules prefill and decode stages *independently*, using a Dispatcher for prefill-stage tasks and a Migrator for decode-stage tasks, ensuring proactive SLO compliance and improved resource utilization. Evaluation shows that HyperFlexis improves SLO attainment by up to **4.44 $\times$** , reduces latency by up to **65.82%**, and lowers cost by up to **49.81%**.
- We develop a *unified scaling framework* that supports both collocated and disaggregated execution. The P/D scaling controller dynamically adjusts resources based on load and utilization, enabling seamless role transitions between prefill and decode workers. To further reduce scaling overhead, we introduce a fast scaling mechanism that leverages device-to-device (D2D) model weight transfers, cutting cold-start latency by up to **19.39 $\times$** .

The rest of the paper is organized as follows. Section 2 provides background, and Section 3 formulates the problem. Section 4 presents the overall design of HyperFlexis, followed by detailed discussions of dispatching in Section 5 and scaling in Section 6. Section 7 describes the experimental setup, and Section 8 presents the evaluation results. Finally, Sections 9, 10, and 11 cover the ablation study, related work, and conclusions, respectively.

## 2. Background

### 2.1. Large Language Model & LLM Service

LLMs are deep neural networks trained on vast amounts of text data to perform a variety of natural language processing tasks, such as text generation, summarization, and question answering. Examples include Alibaba’s Qwen [5], and Meta’s LLaMA [42], which represent state-of-the-art open-source models used in research and industry.

LLM inference typically involves two computationally distinct phases: the Prefill phase, which generates the first token using full-sequence attention, and the Decode phase, where subsequent tokens are generated incrementally using cached key–value states. The Prefill phase is both latency-sensitive and compute-intensive due to full attention computation, whereas the Decode phase is more throughput-oriented, benefiting from batching and sparsity techniques [21].

An LLM service generally follows a client–server architecture: the client submits a sequence of text as a request; the server, hosting the LLM on accelerators such as GPUs or NPUs, performs inference over the request and returns (or streams) the generated output to the client. This architecture enables interactive applications such as chatbots, code assistants, and real-time translation services.

## 2.2. Execution Modes: Collocated vs. Disaggregated

LLM serving systems can be deployed under different execution modes, which determine how computational and memory resources are organized to process user requests. In the collocated mode, all stages of inference are executed on the same set of devices, both the compute-intensive prompt phase and the throughput-oriented decode phase. This approach minimizes inter-device communication latency, but can lead to under-utilization when workloads are unbalanced. In the disaggregated mode, computation and/or memory resources are separated across devices or nodes. Disaggregation enables flexible scaling, better resource utilization, and reduced cost for large-scale serving, but introduces additional communication overhead [21, 35, 36].

## 2.3. Ascend NPU

Neural Processing Units (NPUs), including Ascend, are domain-specific accelerator designed for large-scale matrix and tensor operations common in deep learning, often delivering higher performance and energy efficiency than general-purpose CPUs or GPUs [26]. Built on the Da Vinci architecture [27], each AI core integrates a cube tensor engine, vector unit, and scalar unit, all optimized for neural network computation—unlike GPUs, which were originally crafted for graphics and then adapted for general compute. The accompanying CANN software stack [60] supports popular frameworks (e.g., MindSpore, PyTorch) and compiles workloads into optimized operator graphs for the hardware. Ascend NPUs are deployed in both standalone servers and large-scale clusters, such as the CloudMatrix platform, enabling scalable, multi-tenant training and inference for diverse AI applications [19, 58].

## 2.4. Multi-SLOs Serving

An SLO is a measurable performance target that a system aims to achieve, usually based on user experience requirements. In LLM inference, common latency-related SLOs include Time-to-First-Token (TTFT) and Time-Per-Output-Token (TPOT). TTFT measures the elapsed time from when a request is issued to when the first token is generated. It mainly depends on the latency-sensitive prompt phase and is critical for interactive applications such as chatbots. TPOT measures the average time taken to generate each subsequent token after the first. This metric is influenced by the decode phase and affects throughput.

Multi-SLO serving refers to handling workloads where different requests have distinct SLO targets. Supporting multiple SLOs in the same system is challenging because optimizing for one metric can degrade the other. Without multi-SLO awareness, a system may over-provision resources for low-priority requests or starve latency-critical ones, leading to poor user experience and inefficient utilization [7, 21, 53].

## 3. Problem Formulation

In this section, we formalize a dynamic, latency-aware scheduling and scaling problem for LLM serving under heterogeneous and unpredictable request arrivals, while balancing two competing goals: (1) Minimizing NPU usage cost. As computing resources are expensive, overprovisioning directly impacts operating expenses. (2) Maximizing user satisfaction. Users expect strict SLOs for TTFT and TPOT, especially in interactive applications. Achieving both requires real-time

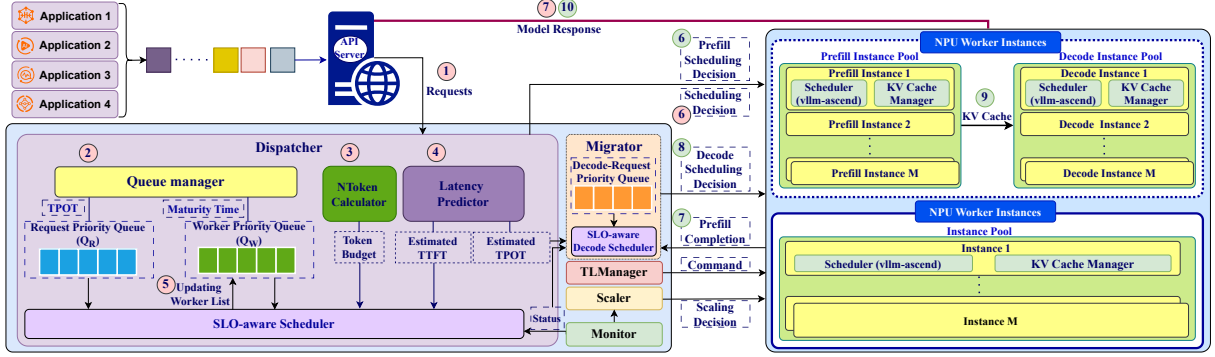


Figure 1 | **Overview of HyperFlexis’s LLM serving architecture and request flow.** A client request enters through the API Server (1) and passes through the Dispatcher’s Queue Manager (2). The Scheduler uses the N-token Calculator (3), Latency Predictor (4), and Monitor status to make a scheduling decision, update the Worker List (5) and send the Decision to workers (6). In collocated execution (red path), after the execution, the Model Response (7) is sent back to the API Server. In P/D disaggregated execution (green path), the Dispatcher schedules the prefill stage (6), and after Prefill Completion (7), the Migrator schedules the decode stage (8), transferring KV cache (9) via the TLManger before decoding. Once decoding completes, the Model Response (10) is returned. The Scaler continuously monitors the system and triggers scaling in or out through the TLManger.

decisions about scaling and dispatching, and stage-dependent processing characteristics.

The system receives a stream of  $M$  requests, denoted by  $R = \{r_1, \dots, r_M\}$ . A request  $r_m$  arriving at  $T_{\text{arrival}}(r_m)$  is characterized by input length  $l^{\text{in}}(r_m)$ , output length  $l^{\text{out}}(r_m)$ , and service-level objectives  $\text{TTFT}(r_m)$  and  $\text{TPOT}(r_m)$ . These attributes jointly determine the computational demand imposed on the serving system and the likelihood of meeting user-specified SLOs.

Requests are dispatched to NPU workers  $W = \{w_1, \dots, w_N\}$ , where  $N$  is bounded by cluster resource availability. Each request progresses through two distinct stages: the prefill stage and the decode stage.

In the prefill stage, the prompt is processed in its entirety prior to output generation. Specifically, given a prefill batch  $\{r_1, \dots, r_B\}$ , the prefill latency  $E_p$  can be estimated [57] by

$$E_p = a + b \sum_{m=1}^B l^{\text{in}}(r_m) + c \sum_{m=1}^B (l^{\text{in}}(r_m))^2, \quad (1)$$

where the coefficients are empirically profiled. The quadratic term accounts for the superlinear growth in latency with large prompt lengths. In the decode stage, output tokens are generated incrementally. The per-step latency for a decoding batch is given by

$$E_d = a' + b' \sum_{m=1}^B l^{\text{cur}}(r_m) + c' B, \quad (2)$$

where  $l^{\text{cur}}(r_m)$  denotes the current length of request  $r_m$ , defined as the number of prefill and decoded tokens so far. The term  $c' B$  captures batching effects on decoding efficiency.

System-level performance is evaluated from two complementary perspectives. From the cost perspective:

$$\text{Cost} = \sum_{n=1}^N (\text{active time of worker } n) \cdot \text{UnitCost}, \quad (3)$$

where  $\text{UnitCost}$  denotes the cost of renting a worker per second. From user perspective, the satisfaction can be measured by

$$\text{Attainment} = \frac{1}{M} \sum_{m=1}^M \mathbb{I}_{\text{TTFT}}(r_m) \cdot \mathbb{I}_{\text{TPOT}}(r_m), \quad (4)$$

where  $\mathbb{I}_{\text{TTFT}}(r_m)$  denotes whether TTFT requirement is met, and similar for TPOT. Other user-centric metrics can also be considered, e.g., the end-to-end latency for request  $r_m$  is  $L_{\text{E2E}}(r_m) = T_{\text{complete}}(r_m) - T_{\text{arrival}}(r_m)$ .

The decision problem is to determine, at each event (request arrival or prefill/decode completion), both (i) whether to adjust the number of active workers and (ii) how to assign pending requests to available workers. Key challenges include balancing batching for NPU efficiency with SLO compliance, coordinating prefill/decode stages to avoid contention, proactive scaling under model startup delays, and adapting to unpredictable workloads. These considerations motivate real-time scheduling and scaling decision-making that explicitly incorporates stage-level latency modeling and trade-offs between cost and attainment.

## 4. HyperFlexis Overall System Design and Framework

In this section, we present the overall system design and framework of HyperFlexis as illustrated in Figure 1.

We present our design based on two guiding principles:

1. Locally, we ensure that each worker adheres to SLOs for its requests, maximizing the number of requests it can process without violating these constraints.
2. Globally, a scaler makes scaling decisions based on the current system state, scaling out to handle urgent requests and scaling in during under-utilization.

At a high level, multiple client applications submit LLM inference requests with heterogeneous latency targets, including TTFT and TPOT. These requests enter the system through an API server and are managed by the centralized **Multi-SLO-Aware Dispatcher** (§5). The dispatcher classifies requests by SLO type and enqueues them in a Request Priority Queue. Leveraging system status information from the **Monitor**, and using available token budgets and predicted latencies, it determines which requests to dispatch. A Worker-Priority Queue predicts worker availability and assigns requests, ensuring that new assignments do not violate the SLOs of either new or ongoing requests.

Execution proceeds differently depending on the deployment mode. In a collocated configuration, dispatched requests are executed on workers and results are returned directly to clients through the API server. In a P/D disaggregated setting, scheduling is split into two stages: (i)

prefill requests are scheduled to prefill workers according to TTFT constraints, and (ii) decode requests are later migrated and scheduled by the **Migrator** based on TPOT priorities. The **TransferLink Manager (TLManager)** coordinates this migration by transferring KV cache data between workers.

Resource provisioning is managed by a **Scaling Controller** (§6), which supports both disaggregated and collocated deployments. It dynamically adjusts worker counts based on real-time metrics such as utilization and queue states. The Scaling Controller also enables seamless role transitions between prefill and decode workers.

To further improve scalability, HyperFlexis integrates a fast scaling mechanism using the **TLManager**. Instead of loading model weights from storage, weights are transferred directly from an already running instance via a high-bandwidth D2D link, significantly reducing cold-start latency.

The **Monitor** subsystem underpins these mechanisms by continuously collecting statistics on worker utilization, request latencies, queue states, and worker roles. This data feeds into both scheduling and scaling decisions.

In summary, HyperFlexis unifies multi-SLO-aware scheduling, disaggregated prefill/decode execution, and fast, role-adaptive scaling into a single system. It ensures efficient resource use while meeting diverse latency objectives. In the following section, we elaborate on how these mechanisms are realized in practice.

## 5. Dispatching Mechanism and Policy

### 5.1. SLO-Aware Dispatching Mechanism.

SLO-aware dispatching must balance two goals: (i) admitting new requests promptly so urgent work begins without delay and (ii) protecting in-flight requests to meet their SLOs. We use a centralized dispatcher to avoid the coordination overhead and suboptimal placements of decentralized schemes, where each worker selects from requests. Our design prioritizes ongoing requests and admits new ones only when workers can safely accommodate them, determined by a maturity time that indicates when a worker can accept additional load without risking deadlines. By maintaining and updating maturity times centrally, the dispatcher enables low-overhead global scheduling that preserves SLOs while admitting new requests as early as possible.

**Collocated Architecture.** The Dispatcher module maintains a global queue of incoming requests ( $Q_R$ ), prioritized first by SLO requirements and then by arrival time. The scheduling process proceeds in five steps: (1) *Select a worker*. The dispatcher selects the earliest available worker from a priority queue ( $Q_W$ ) ordered by maturity time. Maturity time is centrally computed using per-worker latency models and updated worker state; after each dispatch, it is recalculated immediately, with periodic telemetry from the monitor used to correct delayed observations. (2) *Compute token budget*. For the chosen worker, the dispatcher calculates its token budget  $n_{\text{token}}$ , which bounds how many tokens can be generated without violating any SLOs

$$n_{\text{token}} \leq \frac{\text{TTFT} \cdot \text{TPOT} - \text{TTFT} \cdot E_d - a \cdot \text{TPOT}}{b \cdot \text{TPOT}} \quad (5)$$

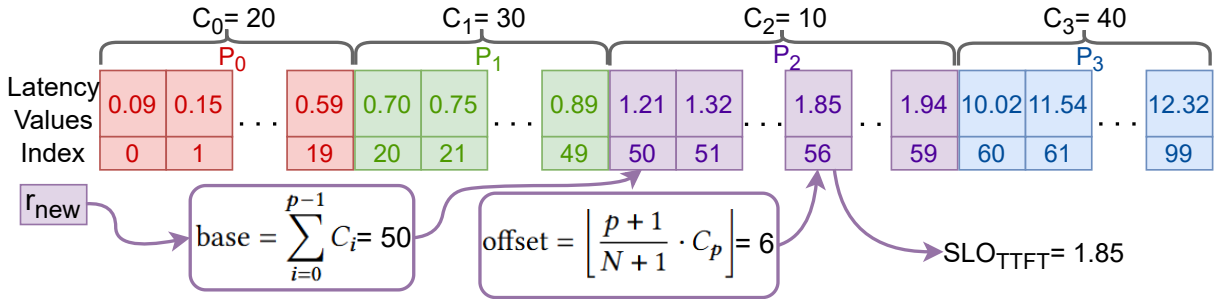


Figure 2 | Priority-based SLO mapping example.  $SLO_{TTFT}$  is determined from recent performance data.

where TTFT and TPOT denote the tightest latency targets,  $E_d$  is the estimated decode cost of ongoing requests, and (a, b) are coefficients from the latency model. This computation ensures that the requests assigned to each worker comply with the SLOs. (3) *Scan the request queue*. The dispatcher scans  $Q_R$ , which is sorted by TPOT and arrival time, to identify candidate requests  $\mathcal{R}$  that could fit within the token budget. (4) *Admit feasible requests*. For each candidate, the dispatcher estimates the probability of meeting its TTFT constraint given its waiting time, TTFT target, estimated prefill duration, and current worker utilization. Only requests whose probability exceeds a predefined threshold are admitted into the  $\mathcal{R}$ . (5) *Dispatch and update state*. Then  $\mathcal{R}$  will be dispatched to the selected worker. The worker’s maturity time is updated based on the predicted processing duration under the new workload and reinserted into the  $Q_W$ . The dispatcher also updates its local shadow state for that worker before moving on to the next available one.

This step-by-step process ensures that urgent requests are admitted promptly while preventing overload, preserving capacity for future high-priority arrivals. The pseudo code for this algorithm is provided in Algorithm 1.

**PD-Disaggregated Architecture.** In P/D-disaggregated configuration, we have separate worker pools for prefill ( $P$ ) and decode ( $D$ ). Therefore, independent schedulers for each stage are used based on Algorithm 1, with the  $P$ -stage handling incoming prefill requests using previous Dispatcher and the  $D$ -stage processing prefilled requests will be handled by Migrator module.

This two-stage scheduling contrasts with existing systems that often use one-shot dispatching, assigning both prefill and decode instances as soon as a request arrives. One-shot dispatching suffers from two main drawbacks: (i) prefill completion times are hard to predict due to queuing delays, and (ii) decode-stage workload distribution is uncertain, potentially causing SLO violations. Two-stage, multi-SLO-aware dispatching addresses these issues by decoupling scheduling into two modules: the Dispatcher for prefill-stage and the Migrator for decode-stage, isolated in separate processes but sharing instance workload state. This separation prevents performance interference, naturally balances CPU usage, and is particularly beneficial on Ascend servers with ARM cores that have limited single-thread performance.

For maturity time, in the  $P$  stage, since a prefill step in static batching is non-interruptible, we set the next maturity interval of an instance to the time when its next prefill batch is completed. In the  $D$  stage, workers can be interrupted at each decode iteration. We estimate the time for the next decoding step and make decisions at every iteration.

---

**Algorithm 1:** SLO-aware Dispatcher (adaptive interval based on SLO)

---

**Attribute** *Request Priority Queue*  $Q_R$ : A queue that stores incoming requests based on their (TPOT, arrival time).

**Attribute** *Worker Priority Queue*  $Q_W$ : A queue that maintains the states of all workers (i.e., instances), ordered by their next available (maturity) time.

**Function** *OnRequestArrive*(*request r*):

- // Triggered when a new request arrives.*
- Add *r* to the  $Q_R$  according to its task type;

**Function** *Init*():

- Start *RunInBackground*() and *Dispatcher*() coroutines, and add them to the event loop;

**Function** *calculate\_p*(*r*):

- $t_{\text{remaining}} \leftarrow (\text{arrival\_time}(r) + \text{TTFT}(r)) - (\text{now} + \text{Expected}_{\text{prefill}}(r))$ ;
- return** *p* based on  $t_{\text{remaining}}$  and resource utilization mapped to range  $[0, 1]$

**Function** *get\_ntoken*(*w*):

- // calculate max number of token without SLO violation.*

**Coroutine** *RunInBackground*():

- while** *True* **do**
  - await sleep for interval time  $T$ ;
  - Synchronize with the current states of local workers;

**Coroutine** *Dispatcher*():

- while** *True* **do**
  - // Select the worker with the earliest maturity time(available time)*
  - $w \leftarrow Q_W.\text{pop}()$
  - // Free tokens for each worker are collected during synchronization*
  - $\text{token\_limit} \leftarrow \min(\text{free\_token}(w), \text{get\_ntoken}(w))$ ;
  - New requests to dispatch  $\mathcal{R} \leftarrow \emptyset$ ;
  - // Prioritize requests from stricter SLO.*
  - for** *request r*  $\in W_R$  **do**
    - if*  $\text{calculate\_p}(r) \geq \theta$  *and* (*#tokens in r + #tokens in R < token\_limit*)
      - then**
        - Add request *r* to  $\mathcal{R}$ ;
  - Dispatch  $\mathcal{R}$  to worker *w*, and update worker states and our local worker's state accordingly;
  - // Compute the next wake-up time for worker w to optimize scheduling. Calculate expected prefill latency  $E_p$*
  - $E_p \leftarrow f(\mathcal{B}^{\text{wait}} \cup \mathcal{R}; \text{a prefill step})$ ;
  - $E_d \leftarrow f(\mathcal{B}^{\text{wait}} \cup \mathcal{R} \cup \mathcal{B}^{\text{run}}; \text{a decoding step})$  ; *// Calculate future decoding latency*
  - $\text{relax} \leftarrow \min\{\text{TPOT}_r \mid r \in \mathcal{B}^{\text{wait}} \cup \mathcal{R} \cup \mathcal{B}^{\text{run}}\} - E_d$  ; *// Future time-saving in each decoding iteration*
  - Worker *w* next maturity time  $\leftarrow$  current time  $+ E_p + \frac{E_p}{\text{relax}} E_d$ ;
  - $Q_W.\text{push}(w)$  ;
  - $w' \leftarrow Q_W.\text{peek}()$  ; *// Select the next worker from worker priority queue*
  - await  $w'.\text{mature\_time} - \text{now}$  ; *// Sleep till the next worker w' is available*

## 5.2. Priority-Based SLO Mapping

We design a priority-based SLO mapping scheme to handle cases where users cannot specify explicit metrics such as TTFT or TPOT. In real deployments, customers often lack precise latency targets, but they can usually express the relative importance of their applications. Our scheme leverages these priorities to derive latency SLOs dynamically, adapting them over time as the system operates. This is illustrated in Figure 2 and explained below with five steps.

(1) *Priority as input.* Each request is assigned a priority  $p$ , with 0 being the highest and  $N - 1$  the lowest, with  $N$  representing the total number of priority levels. (2) *Sliding-window history.* The system maintains two sliding windows of size  $W$  for recent TTFT and TPOT values. Each new result is inserted while the oldest entry is dropped, ensuring SLOs are based on up-to-date conditions. (3) *Mapping priority to latency.* For each new request ( $r_{\text{new}}$ ), the system determines its SLO latency within the window using an indexing scheme. The base index accounts for all higher-priority requests already placed in the window, while the offset determines the request's position within its own priority class. This mapping biases higher priorities toward lower-latency quantiles and lower priorities toward higher-latency quantiles. Formally:

$$\text{base} = \sum_{i=0}^{p-1} C_i, \quad \text{offset} = \left\lfloor \frac{p+1}{N+1} \cdot C_p \right\rfloor \quad (6)$$

where  $C_i$  is the count of completed requests with priority  $i$  in the window. The sum ( $i_s = \text{base} + \text{offset}$ ) indexes the latency used as the provisional SLO for  $r_{\text{new}}$ . (4) *Correcting for queuing effects.* To prevent temporary queue spikes from inflating SLOs, we subtract the extra queuing delay between the chosen reference request and the most recent request of the same priority. This correction keeps SLOs aligned with real-time system behavior. (5) *Ensuring stability.* Derived SLOs are bounded within pre-defined ranges per priority. A contention-aware rule further stabilizes outcomes: If higher-priority requests are pending, the system enforces the strict lower bound. Otherwise, the bound is relaxed so lower-priority requests may complete sooner without undermining priority ordering.

Finally, the adjusted TTFT and TPOT values are delivered to the SLO-aware scheduler (Algorithm 1) for integration into dispatching decisions.

## 6. Scaling Mechanism and Policy

To mitigate SLO violations from insufficient resources, we design a threshold-based scaling mechanism (Algorithm 3). The *Scaler* module executes every  $\tau$  seconds, monitoring worker utilization, request wait times (relative to their SLOs), input queue rates, and system processing rates. If any of these metrics exceed an upper threshold  $\epsilon_o$ , additional workers are provisioned. Conversely, if they remain below a lower threshold  $\epsilon_i$  for a sustained period, workers are decommissioned to improve cost efficiency.

Scaling in disaggregated P/D deployments requires additional considerations. Because prefill and decode workloads differ in generation length and SLO requirements, our system independently scales each phase and dynamically reassigns workers across roles when their demand diverges. This role reconfiguration avoids unnecessary instance churn. To enable it, vLLM-Ascend engines are role-agnostic and communicate through flexible P/D links that support

---

**Algorithm 2:** Priority-Based SLO Assignment

---

**Input:** Request  $r_{new}$  with priority  $p \in [0, N-1]$   
**Output:** Assigned SLOs for request  $r_{new}$   
**Attribute  $ttft\_records$  and  $tpot\_records$ :** Sorted sliding windows of recent request SLOs (size  $W$ )  
**Attribute  $C_0, C_1, \dots, C_{N-1}$ :** Counts of requests per priority in sliding window  
**Attribute  $last\_queue\_time$ :** Last observed queue time list for each priority

```
// Retrieve TTFT and TPOT from sliding windows
idx ← get_priority_index(p, C[0 : N - 1]);
(ttft, q_time) ← ttft_records[idx];
tpot ← tpot_records[idx];
// Adjust TTFT to reduce impact of queue time spikes
Δqueue_time ← q_time - last_queue_time[p];
ttft ← ttft - Δqueue_time;
last_queue_time[p] ← q_time;
// Retrieve and clamp TTFT and TPOT
ttft ← clamp(ttft, min_ttft(p), max_ttft(p));
tpot ← clamp(tpot, min_tpot(p), max_tpot(p));
return (ttft, tpot);
```

---

bidirectional KV data transfer. The *TLManager* proactively establishes these links when new workers are added, ensuring immediate traffic handling and avoiding the latency of on-demand setup as in Mooncake [33].

**Fast Scaling** A major challenge in scaling is cold-start latency, since loading large model weights from disk take time if not cached in memory. To address this, we introduce *Fast Scaling*, a two-stage weight provisioning design. First, a warm-up pool of instances is pre-initialized: each launches its CPU runtime but delays weight loading, with the pool size defaulting to the maximum number of devices. Each running instance includes a WeightManager that maps tensor names to memory pointers, enabling them to act as weight sources. During scaling, the *TLManager* selects a source instance, sets up a temporary communication domain, and maps devices based on topology. The target issues asynchronous receive\_weight requests while the source performs send\_weight operations, transferring data tensor-aligned and device-to-device. After completion, the target moves from the warm-up to the running pool; on failure, the system falls back to disk loading. This approach reduces cold-start latency while preserving reliability.

## 7. Experimental Setup

We evaluate HyperFlexis on different models, realistic hardware constraints, and representative multi-SLO workloads. Unless otherwise noted, all methods are tested under identical hardware, software, and workload configurations to ensure a fair comparison. Each experiment is repeated three times, with the mean shown as point and the standard deviation represented as error bars in the plots.

---

**Algorithm 3:** SLO-Aware Scaling (High-Level)

---

**Input:**  $Utils$ : list of workers utilization,  
 $T_{wait}$ : list of request wait times relative to SLOs,  
 $R_{In}$ : rate of incoming requests,  
 $R_{Process}$ : rate at which requests are processed  
**Attribute**  $\tau$ : scaling interval,  
 $\epsilon_o$ : upper threshold for scaling out,  
 $\epsilon_i$ : lower threshold for scaling in;  
**while** True **do**  
    **if** time since last scaling decision  $\geq \tau$  **then**  
        // Compute overall system load metric  
         $LoadMetric \leftarrow f(Utils, T_{wait}, R_{In}, R_{Process})$   
        **if**  $LoadMetric > \epsilon_o$  **then**  
            scale\_out();  
            // Add worker  
        **if**  $LoadMetric < \epsilon_i$  **then**  
            scale\_in();  
            // Remove worker

---

## 7.1. Environment

We conducted all experiments on a cluster of four servers. Each server is equipped with eight Ascend NPUs [25], each providing 64 GB of memory. Additionally, each server contains four HiSilicon Kunpeng-920 CPUs [49], with 48 cores per CPU (192 cores in total), running in 64-bit ARMv8-A mode (aarch64). Our implementation is built upon PyTorch 2.1.0 [4] with the Ascend backend, Python 3.9.9, CANN 7.6 [24], and vLLM-Ascend [44].

## 7.2. Serving Models

We evaluate our system using three representative open-source LLMs: Qwen7B and Qwen32B [5], and Llama70B [42]. These models span a wide range of deployment scales, from lightweight setups to large-scale deployments. All experiments are conducted with FP16 or BF16 precision, the standard configuration for inference serving as it balances efficiency and accuracy. We employ tensor parallelism [37] (TP) to distribute weights across devices, using TP=1 for Qwen7B, TP=2 for Qwen32B, and TP=8 for Llama70B.

## 7.3. Benchmark Workloads and Datasets

We evaluate our approach using two distinct multi-SLO task sets. The first set contains four diverse tasks with heterogeneous SLO requirements, summarized in Table 1. This set includes the `medical_qa` dataset [12], which consists of auto-generated answers to clinical medical questions; the `tldr_content_gen` and `tldr_headline_gen` datasets [54], which focus on text generation by producing article content from headlines and headlines from article content, respectively; and the `wikisql` dataset [54, 56], a semantic parsing benchmark mapping natural language questions to SQL queries over tables. The second set comprises two tasks, `gsm8k` [11] that contains grade school math word problems and `sharegpt` [55] that is a collection of conversational data, representing high-complexity reasoning and conversational AI workloads,

Task	SLO (s)		Lengths	
	TTFT	TPOT	Input	Output
medical_qa [12]	0.7	0.5	$32.57 \pm 10.32$	$38.92 \pm 16.83$
tldr_content_gen [54]	1	0.7	$44.38 \pm 6.58$	$96.04 \pm 35.03$
tldr_headline_gen [54]	2	0.9	$121.82 \pm 35.04$	$13.59 \pm 6.55$
wikisql [54]	20	1	$643.22 \pm 337.01$	$27.82 \pm 4.84$
gsm8k [11]	0.7	0.2	$51.44 \pm 15.78$	$90.13 \pm 26.73$
sharegpt[55]	2	0.5	$259.19 \pm 324.88$	$207.79 \pm 234.99$

Table 1 | **Summary statistics of the benchmark tasks.** The first four tasks form the 4-task multi-SLO set, and the last two form the 2-task set. Input/output lengths are reported as mean  $\pm$  standard deviation over 300 requests.

respectively.

For evaluation, we draw 300 samples per task. Requests for each task follow a Poisson inter-arrival time distribution, with each task contributing an equal number of samples. A fixed random seed is used to ensure reproducibility.

For priority-based SLO mapping (HyperFlexis-PM), we use the median SLO targets from Table 1 with a  $\pm 25\%$  range to separate priorities while allowing dynamic assignment based on real-time workloads.

#### 7.4. Baselines

We compare HyperFlexis against four scheduling approaches. ALADDIN [30] is a heuristic-based latency optimizer for single-task scenarios. SIMULATED ANNEALING (SA) [18] is a stochastic scheduler for multi-SLO workloads. SCORPIO [40] also targets multi-SLO workloads; we added Round Robin logic to it to support multi-instance scheduling. Finally, we use Llumnix [39] with ROUND ROBIN (RR) as another baseline (referred to simply as RR). These baselines cover both single-task and multi-SLO strategies, enabling evaluation under diverse competitive conditions. Experiments are conducted in the collocated system unless stated otherwise.

#### 7.5. Metrics

We evaluate performance using three metrics (§3): **SLO attainment**, the fraction of requests meeting latency targets; **E2E latency**, the total time from request arrival to token generation; and **Resource cost** (Equation 3), the cumulative *active time* of all instances (one unit = one instance active for 50 ms), capturing both instance count and duration for fair comparison between methods with and without scaling.

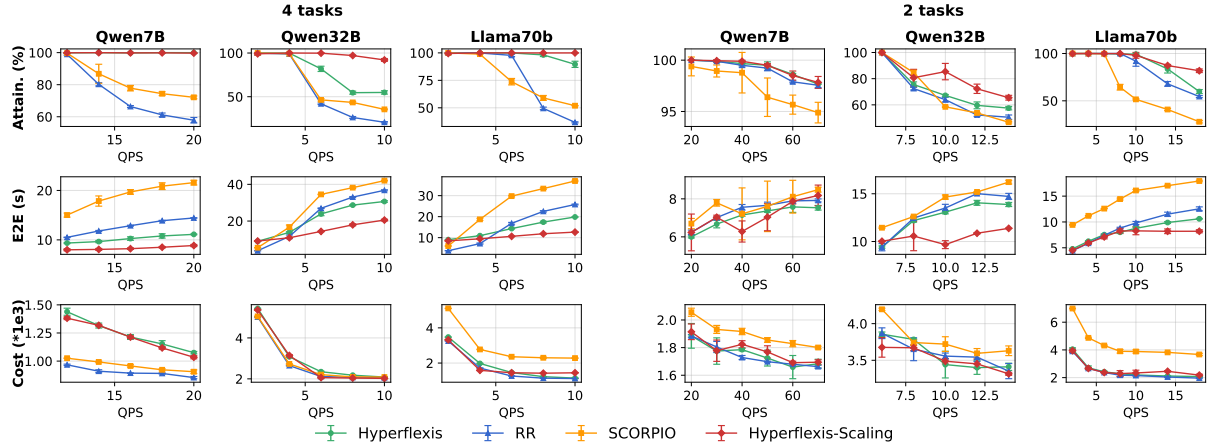


Figure 3 | **Multi-task performance on 2-task and 4-task workloads.** Metrics include SLO attainment (top, higher is better), end-to-end latency (middle, lower is better), and cost (bottom, lower is better) for HyperFlexis, RR, SCORPIO, and HyperFlexis-Scaling. Results use two workers, with up to four for scaling.

## 8. Evaluation

### 8.1. Multi-task Performance Evaluation

#### 8.1.1. Collocated Architecture Results

We first evaluate HyperFlexis under multi-task workloads, with the comparative results shown in Figure 3.

**SLO Attainment** As shown in the upper row of Figure 3, HyperFlexis and HyperFlexis-Scaling consistently achieve higher SLO attainment than both RR and SCORPIO, with the gap widening at higher query-per-second (QPS). In the 4-task benchmark, HyperFlexis improved attainment by up to  $2.60\times$  over RR and  $1.73\times$  over SCORPIO, while HyperFlexis-Scaling achieved up to  $4.44\times$  and  $2.59\times$ , respectively. In the 2-task benchmark, the improvements were  $1.23\times$  and  $2.14\times$  for HyperFlexis, and  $1.5\times$  and  $2.93\times$  for HyperFlexis-Scaling. As the number of tasks increases, the benchmark becomes more complex, underscoring the need for an SLO-aware scheduling algorithm that can efficiently allocate resources and sustain high SLO attainment under diverse conditions.

**End-to-End Latency** Second row of Figure 3 shows that while all methods have similar latency at low QPS, our advantages become apparent as the load increases. For Qwen7B on the 2-task benchmark, attainment is similar across methods, but we achieve up to 16.85% lower latency than RR and 12.58% lower than SCORPIO. Compared to SCORPIO, HyperFlexis achieves up to 54.26% improvement (latency reduction) with scaling and 49.21% without scaling. On the 4-task benchmark, our method achieves up to 23.03% and 51.91% improvement over RR and SCORPIO, respectively, with scaling further increasing these numbers to 50.96% and 65.82%. These results demonstrate that HyperFlexis’s SLO-aware scheduling effectively mitigates queuing and contention, maintaining responsiveness under heavy load.

**Cost Efficiency** Figure 3’s bottom row compares cost across workloads. On the 2-task benchmark, we observed similar cost to round-robin, with occasional slight reductions of up to

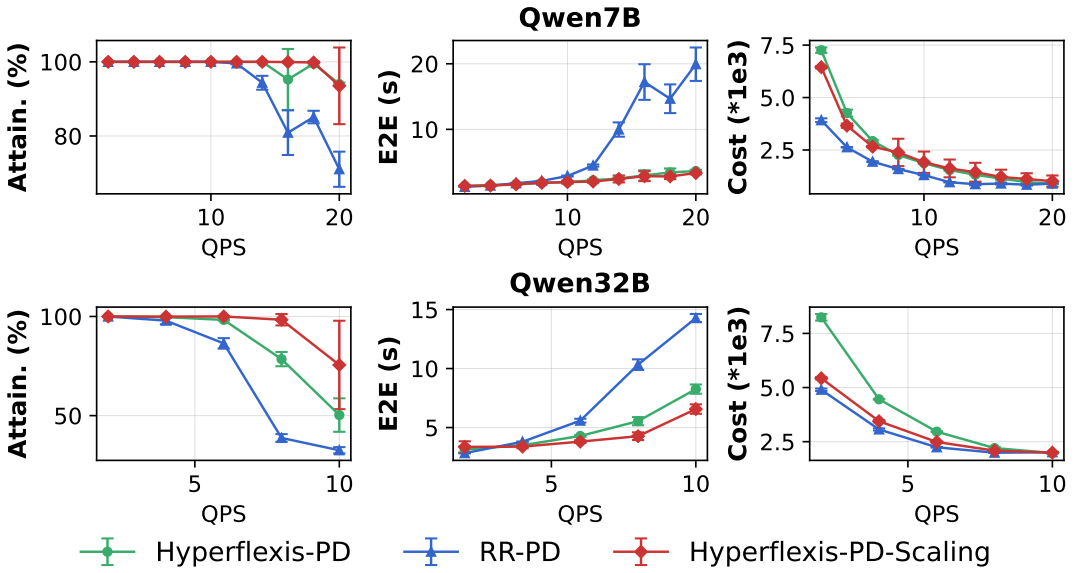


Figure 4 | **Performance comparison under P/D disaggregated mode.** Results for 4-task workloads using Qwen7B and Qwen32B.

4.99%. Compared to SCORPIO, HyperFlexis achieves cost reductions of up to 44.46% without scaling and 45.29% with scaling. On the 4-task benchmark, smaller model incurs a higher cost by improving attainment and lower latency. However, for larger models, we achieve a comparable cost to RR, and for Llama70B, we observe up to 49.81% improvement over SCORPIO.

Overall, HyperFlexis and HyperFlexis-Scaling consistently outperform RR and SCORPIO in terms of SLO attainment, end-to-end latency, and cost efficiency. SLO-aware scheduling enables significant improvements in attainment, particularly under high load and complex multi-task scenarios, while simultaneously reducing latency by up to 65.82% and achieving substantial cost savings compared to SCORPIO.

### 8.1.2. P/D Disaggregated Architecture Results

Figure 4 shows the comparison under the P/D Disaggregated Mode for a 4-task workload. For HyperFlexis-PD-Scaling, we initially allocate 4 instances (2 Prefill and 2 Decode instances) and allow scaling up to 8 instances on demand. Note that the experiment for Qwen32B (TP=2) runs across nodes, highlighting the system’s scalability and flexibility. The RR-PD baseline means that request dispatching in both the Prefill and Decode stages follows a round-robin policy. As shown in the Figure 4, both HyperFlexis-PD and HyperFlexis-PD-Scaling achieve higher attainment (up to 2.54×) and lower request latency (up to 31.82% reduction) compared to RR-PD. With auto-scaling enabled, the cost of HyperFlexis-PD-Scaling is only slightly higher than RR-PD for Qwen7B and roughly equivalent to RR-PD for Qwen32B.

## 8.2. Priority Mapping Results

We evaluate HyperFlexis’s performance using priority-based mapping on Qwen models across both 2-task and 4-task workloads, as shown in Figure 5.

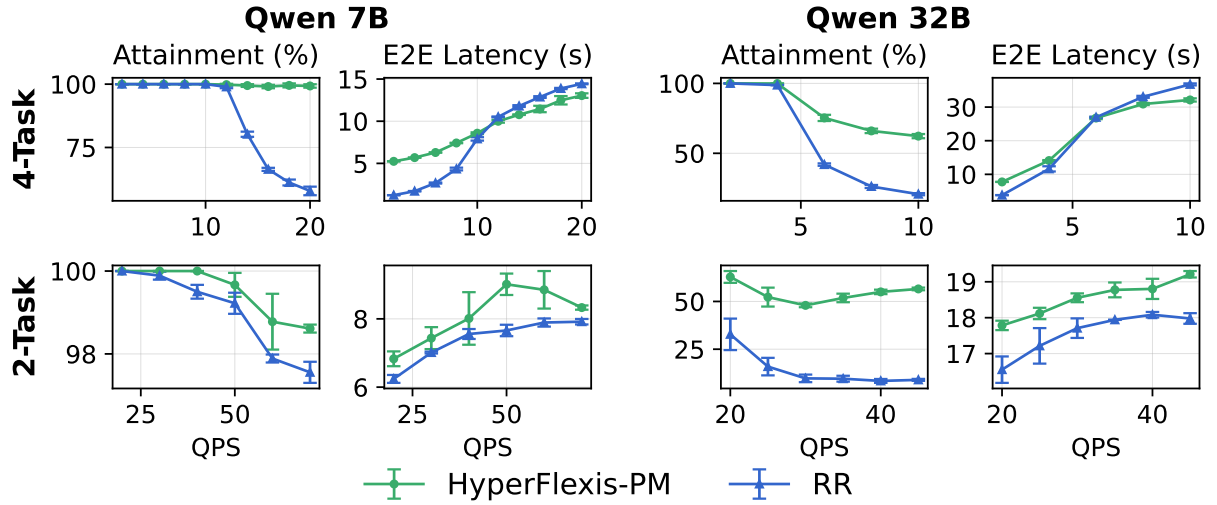


**Figure 5 | Performance of HyperFlexis-PM under dynamic SLO ranges.** Results for 2-task and 4-task workloads using Qwen7B and Qwen32B. Metrics shown are SLO attainment and end-to-end latency comparing HyperFlexis-PM against RR. HyperFlexis-PM consistently achieves higher SLO attainment, especially at higher QPS.

As shown in Figure 5, HyperFlexis consistently outperforms RR in SLO attainment across all workloads, with the advantage increasing at higher QPS due to its multi-SLO-aware scheduling and predictive mechanisms, achieving up to  $7.02\times$  improvement in attainment. Latency varies with workload and load: for 2-task sets, HyperFlexis incurs slightly higher latency due to scheduling overhead and conservative resource allocation with at most 1.35s, whereas for 4-task sets at high QPS, it reduces latency through efficient dispatching, prioritization, and lower queuing delays. The cost metric, which reflects scaling overhead, is not shown here. In general, HyperFlexis with priority-based mapping achieves superior SLO attainment while maintaining reasonable latency.

### 8.3. Fast Scaling Evaluation

We evaluated three scaling strategies for HyperFlexis LLM serving: (1) loading weights from disk when scaling, (2) offloading weights to CPU when scaling out and reloading from CPU when scaling in, and (3) loading weights from an already running instance, which we term *Fast Scaling*. As shown in Table 2, Fast Scaling significantly reduces scaling time, achieving up to a  $9.88\times$  speedup over CPU offloading and  $19.39\times$  speedup over disk-based loading. This demonstrates that reusing memory-resident weights can dramatically accelerate dynamic scaling without incurring the overhead of disk or CPU transfers.

## 9. Ablation Study

### 9.1. Impact of Dynamic SLO Assignment

To evaluate our system’s ability to dynamically adapt to runtime conditions by mapping priorities to absolute SLOs (Section 5.2), we conduct experiments under a dynamic workload.

	Qwen 7B	Qwen 32B	Llama 70B
Fast Scaling	<b>0.89 ± 0.01</b>	<b>2.05 ± 0.02</b>	<b>1.16 ± 0.05</b>
CPU Offloading	2.73 ± 0.17	19.41 ± 3.14	11.50 ± 1.86
Disk loading	4.14 ± 0.26	28.84 ± 2.23	22.58 ± 0.82

Table 2 | **Scaling time for different models.** Results for Qwen7B, Qwen32B, and LLaMA70B using different methods, measured in seconds.

**Dynamic Task Rate** We begin with a single client generating 250 requests lowest-priority tasks (P3 tasks) at 15 QPS. After 20 seconds, a new client joins, issuing P2 tasks at the same rate. This process continues until all four priority levels are active, at which point the total task rate reaches 60 QPS after 60 seconds. The bottom row of Figure 6 shows the resulting stacked request histogram.

In this experiment, absolute task SLOs are derived from Table 1, and HyperFlexis’s priority mapping is configured to satisfy these targets.

As shown in the upper row of Figure 6, RR schedules requests as quickly as possible, creating contention when multiple task types coexist (60–90s window), causing the TTFT of higher-priority tasks to violate their SLOs (blue dotted line).

In contrast, HyperFlexis dynamically adjusts its scheduling. When the system is underloaded (first 20s), it assigns tighter SLOs to low-priority (P3) requests to minimize their latency. As higher-priority requests join and contention increases, HyperFlexis adapts by relaxing the SLOs for lower-priority tasks up to their configured maximum, thereby preserving capacity to meet the strict SLOs of higher-priority tasks.

The results demonstrate that HyperFlexis responds effectively to workload dynamics. By dynamically adjusting assigned SLOs, it optimizes latency when capacity is available and ensures strict prioritization under contention, ensuring all tasks meet their configured performance targets.

## 9.2. Single-task Performance Evaluation

To evaluate HyperFlexis in a single-task setting, we run experiments on the WikiSQL workload using Qwen7B and Qwen32B, allowing comparison with existing single-task, single-SLO methods and showing that HyperFlexis is at least as effective. We compare HyperFlexis with two state-of-the-art baselines, ALADDIN and SA, across varying QPS. For this experiment, TTFT and TPOT SLOs are set to 0.7 s and 0.5 s, respectively.

As shown in Figure 7, all systems maintain near-perfect SLO attainment under light load. As QPS increases, however, ALADDIN’s attainment drops sharply once the system approaches saturation, while HyperFlexis sustains higher attainment, particularly at the knee point for Qwen7B (40 QPS).

Figure 7 also reports end-to-end latency. Under higher loads, however, HyperFlexis delivers more stable performance, avoiding the sharp latency spikes observed with SA and ALADDIN (e.g., at 12 QPS on Qwen32B). These results confirm that HyperFlexis’s scheduling and instance-aware queuing mechanisms improve responsiveness and reduce congestion even in single-task

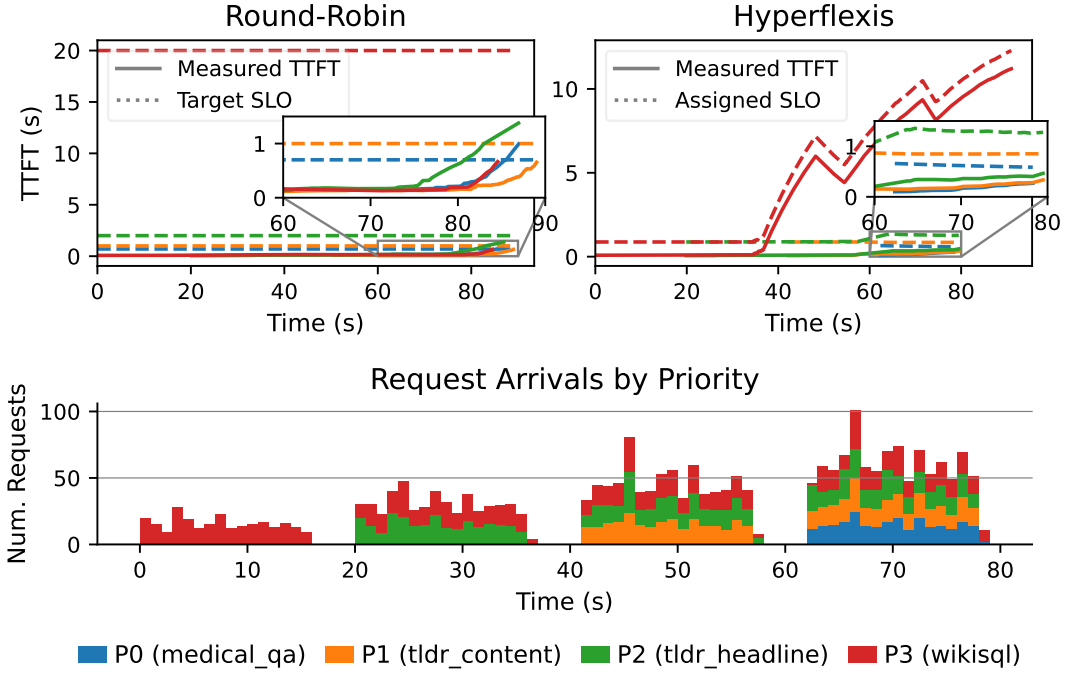


Figure 6 | **Responsiveness of HyperFlexis to dynamic workloads.** Top: The measured TTFT (solid lines) and the TTFT SLO (dotted lines) for different request types, averaged over per-second intervals for the RR (left) and HyperFlexis (right) schedulers. Bottom: The request arrival rate, where P3 starts at 15 QPS and priorities P2–P0 gradually ramp up to a total of 60 QPS at 60 seconds.

settings.

Overall, these results show that although HyperFlexis is designed to handle heterogeneous multi-SLO workloads, it remains competitive with, and in some cases outperforms, ALADDIN and SA in single-task settings. That is, the generality of HyperFlexis does not come at the expense of performance on simpler workloads.

### 9.3. Monitor and Scaling Interval

To understand the sensitivity of HyperFlexis’s performance to key system parameters, we conduct an ablation study varying both the monitoring interval and the scaling interval as shown in Figure 8.

**Effect of Monitor Interval.** We vary the monitor interval across 50 ms, 1 s, and 5 s. As shown in the top row of Figure 8, performance is largely robust to the choice of interval. However, slight trends are observable: (1) SLO attainment is slightly reduced with a 5 s monitor interval compared to 50 ms and 1 s, reflecting delayed feedback that slows adaptation to system status changes; (2) end-to-end latency is marginally higher with the 50 ms interval due to the slight overhead of frequent monitoring, especially under heavy load, though the impact remains minimal. Overall, HyperFlexis is robust across a wide range of monitor intervals, and choosing a moderate interval (e.g., 1 s) provides a good balance between responsiveness and overhead.

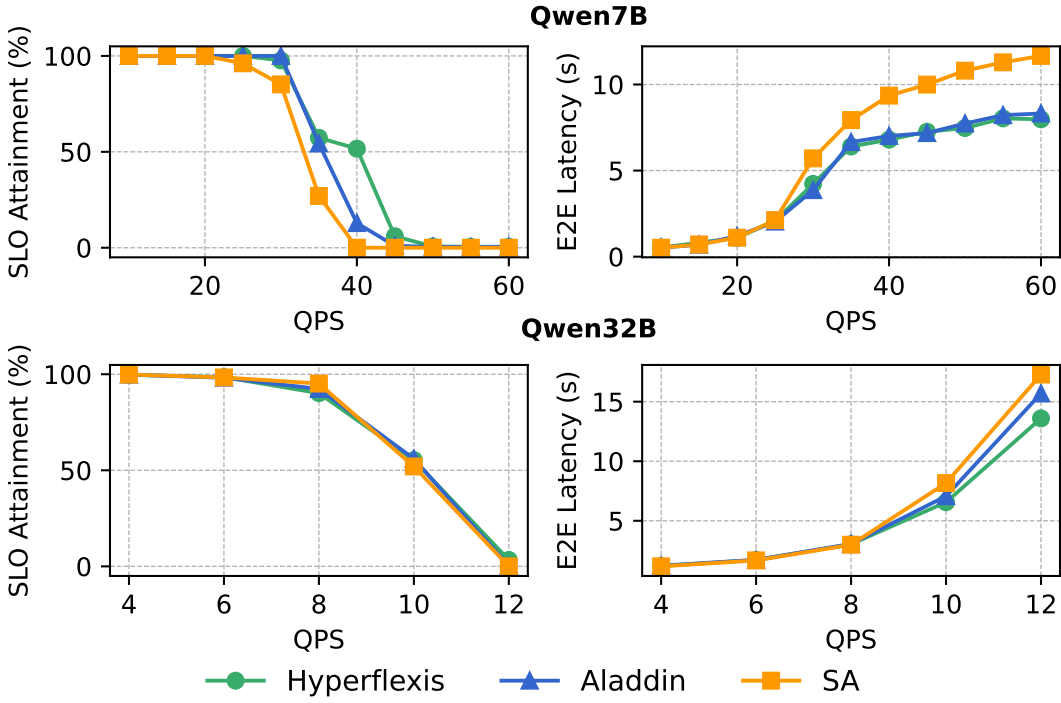


Figure 7 | **Single-task performance comparison.** Results for Qwen7B and Qwen32B on the WikiSQL dataset in compare with Aladdin [30] and SA [18]. The TTFT and TPOT SLOs are set to 0.7 s and 0.5 s, respectively.

**Effect of Scaling Interval.** We vary the scaling interval across 0.5 s, 1 s, and 2 s to evaluate how the frequency of scaling decisions affects performance (Figure 8). SLO attainment shows minimal differences across intervals for most QPS values. At high QPS, shorter intervals exhibit slightly lower attainment, as the overhead of frequent scaling outweighs the benefits, particularly under heavy load when time is critical.

These results suggest that HyperFlexis’s performance is largely insensitive to the scaling interval within the tested range. While very short or intermediate intervals may introduce minor variability in attainment or latency, overall system robustness is preserved.

## 10. Related Works

### 10.1. LLM Inference and Prompt/Decode Separation

Early monolithic systems such as vLLM [21] exploit techniques like PagedAttention for efficient KV reuse in single-GPU settings, but lack explicit SLO-awareness. FlexGen [36] similarly operates on a single node, emphasizing CPU–GPU offloading to reduce memory footprint at the cost of real-time performance. More recent optimizations include Apt-Serve [15], which combines hybrid KV/hidden-state caching with adaptive batch composition to improve TTFT, and Sarathi-Serve [2], which uses chunked-prefill scheduling to saturate GPU compute while bounding Decode latency.

At cluster scale, phase-decoupled systems such as DistServe [57] and Splitwise [31] map

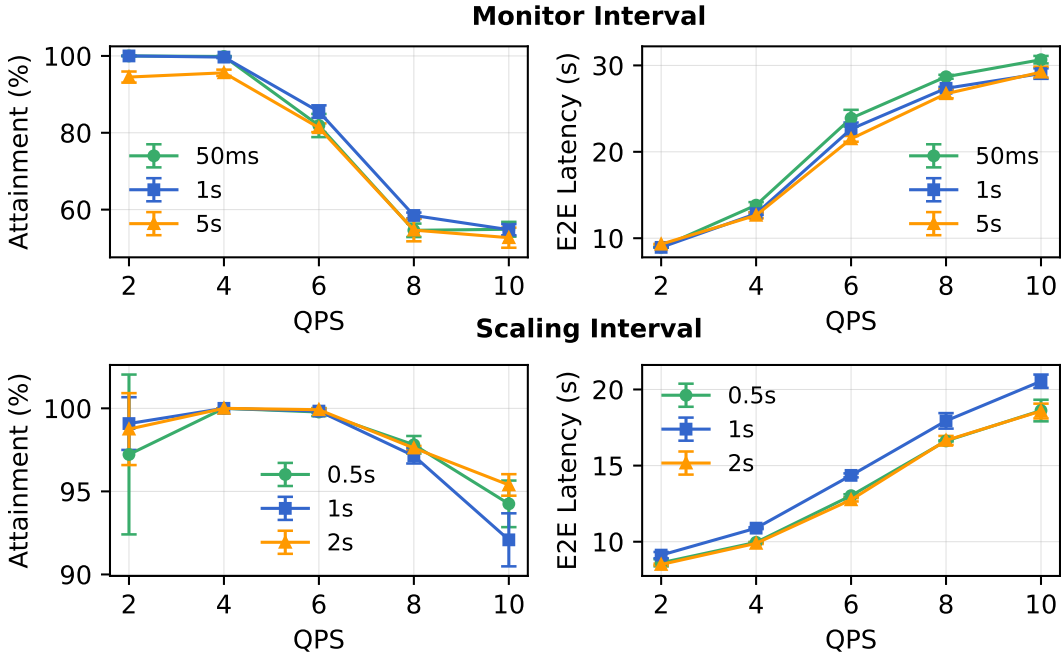


Figure 8 | **Impact of monitor and scaling intervals.** Results for Qwen32B on the 4-task benchmark are shown with two workers (top) and up to four workers (bottom). Overall, HyperFlexis’s performance is largely insensitive to changes in the scaling and monitor intervals.

Prompt and Decode to compute- and memory-optimized nodes, respectively.

LoongServe [45] adapts sequence parallelism to request length, while MIRAGE [23] and BlitzScale [51] improve KV-cache efficiency through remapping and layer-level autoscaling. These systems enhance utilization and tail-latency control, yet multi-SLO-aware scaling and dispatch remain unexplored.

## 10.2. Distributed Multi-SLO Inference Systems

Beyond phase separation, distributed serving frameworks introduce cluster-level scheduling and SLO-aware execution. Llumnix [39] migrates priority requests across instances to reduce latency tails, USHER [38] incorporates interference-aware GPU sharing, and SpotServe [29] resumes preempted workloads at token granularity for spot GPUs. Other designs specialize in scheduling heuristics: ELIS [10] predicts the remaining output length for SRTF scheduling, QLM [32] orchestrates heterogeneous GPUs across multi-model workloads, SCOOT [9] uses Bayesian optimization for single and multi-objective SLOs, and DynaServe [34] introduces micro-request abstraction for adaptive Prompt/Decode balancing. CoCoServe [46] supports fine-grained module-level replication and migration for elastic scaling.

These systems expand the design space from single-node optimization to distributed, SLO-aware serving, but typically treat scaling and placement separately from scheduling.

### 10.3. Multi-SLO Scheduling, Placement, and Scaling

A growing body of work seeks to integrate dispatch, placement, and scaling decisions to meet diverse SLOs. Some approaches extend scheduling with SLO-awareness: Huang et al. [18] use simulated annealing to prioritize by SLO type and input length; SCORPIO [40] combines deadline-based admission control with credit-aware batching; and Tempo [52] applies application-aware scheduling for single-node multi-SLO workloads. However, these either lack phase-decoupled coordination (Tempo) or use static scaling (SCORPIO).

Others target joint optimization in Prompt/Decode (PD) architectures. Arrow [47] dynamically switches between Prompt and Decode execution pools, Aladdin [30] applies best-fit bin packing for joint placement/scaling, and PD-Multiplexing [13] shares Decode workloads to boost throughput. Proteus [3] contributes by dynamically adapting model accuracy to meet throughput demands, trading off precision for performance and significantly reducing latency timeouts compared to baseline approaches. PolyServe [59] and SLOs-Serve [8] incorporate multi-SLO constraints into placement, but rely on offline simulations or fixed thresholds. HAS-GPU [16] enables fine-grained vertical partitioning with hybrid autoscaling, while USHER [38] optimizes throughput/latency holistically across replicas. Yet even these integrated systems often assume slow spin-up times and do not proactively reallocate capacity under bursty load.

In contrast, our work unifies multi-SLO-aware dispatch with dynamic scaling in a both PD-decoupled and collocated architecture.

## 11. Conclusion

We presented HyperFlexis, a unified LLM serving system that addresses the challenges of multi-SLO scheduling and elastic scaling. By combining a multi-SLO-aware dispatcher, a two-stage P/D scheduling mechanism, adaptive SLO mapping, and a fast, unified scaling controller, HyperFlexis efficiently manages heterogeneous workloads across both collocated and disaggregated deployments. It also supports distributed settings, including cross-node scenarios. Our extensive evaluation demonstrates that HyperFlexis significantly improves SLO attainment, reduces latency, lowers operational cost, and accelerates scaling compared to existing baselines. These results show that by integrating SLO-aware dispatching with dynamic scaling, HyperFlexis provides an effective, high-performance, and cost-efficient solution for LLM serving across diverse, multi-task workloads, generalizing across workload sizes, model scales, and deployment architectures to support production-grade, multi-tenant inference systems.

Future work includes exploring heterogeneous models and hardware, enabling HyperFlexis to efficiently serve multiple model types of different sizes and resource requirements on both low-end and high-end hardware simultaneously.

## References

- [1] Josh Achiam, Steven Adler, Sandhini Agarwal, Lama Ahmad, Ilge Akkaya, Florencia Leoni Aleman, Diogo Almeida, Janko Altenschmidt, Sam Altman, Shyamal Anadkat, et al. Gpt-4 technical report. [arXiv preprint arXiv:2303.08774](https://arxiv.org/abs/2303.08774), 2023.
- [2] Amey Agrawal, Nitin Kedia, Ashish Panwar, Jayashree Mohan, Nipun Kwatra, Bhargav S Gulavani, Alexey Tumanov, and Ramachandran Ramjee. Taming throughput-latency tradeoff in llm inference with sarathi-serve. [Proceedings of 18th USENIX Symposium on Operating Systems Design and Implementation](https://www.usenix.org/conference/osdi24/presentation/agrawal), 2024, Santa Clara, 2024.
- [3] Sohaib Ahmad, Hui Guan, Brian D. Friedman, Thomas Williams, Ramesh K. Sitaraman, and Thomas Woo. Proteus: A high-throughput inference-serving system with accuracy scaling. In [Proceedings of the 29th ACM International Conference on Architectural Support for Programming Languages and Operating Systems](https://www.usenix.org/conference/asplos24/presentation/ahmad), Volume 1, ASPLOS '24, page 318–334, New York, NY, USA, 2024. Association for Computing Machinery.
- [4] Ascend Community. Ascend pytorch adapter (torch\_npu). <https://github.com/Ascend/pytorch>. Accessed: 2025-08-18.
- [5] Jinze Bai, Shuai Bai, Yunfei Chu, Zeyu Cui, Kai Dang, Xiaodong Deng, Yang Fan, Wenbin Ge, Yu Han, Fei Huang, et al. Qwen technical report. [arXiv preprint arXiv:2309.16609](https://arxiv.org/abs/2309.16609), 2023.
- [6] Fabian Biester, Mohamed Abdelaal, and Daniel Del Gaudio. LLMclean: Context-aware tabular data cleaning via LLM-generated OFDs. In [European Conference on Advances in Databases and Information Systems](https://www.eurodb.org/eurodb2024/paper/68.pdf), pages 68–78, Cham, Switzerland, 2024. Springer.
- [7] Siyuan Chen, Zhipeng Jia, Samira Khan, Arvind Krishnamurthy, and Phillip B Gibbons. Slos-serve: Optimized serving of multi-slo llms. [arXiv preprint arXiv:2504.08784](https://arxiv.org/abs/2504.08784), 2025.
- [8] Siyuan Chen, Zhipeng Jia, Samira Khan, Arvind Krishnamurthy, and Phillip B. Gibbons. Slos-serve: Optimized serving of multi-slo llms, 2025.
- [9] Ke Cheng, Zhi Wang, Wen Hu, Tiannuo Yang, Jianguo Li, and Sheng Zhang. SCOOT: SLO-oriented performance tuning for LLM inference engines. In [THE WEB CONFERENCE 2025](https://www.thewebconf.org/2025/paper/10.pdf), 2025.
- [10] Seungbeom Choi, Jeonghoe Goo, Eunjoo Jeon, Mingyu Yang, and Minsung Jang. Elis: Efficient llm iterative scheduling system with response length predictor, 2025.
- [11] Karl Cobbe, Vineet Kosaraju, Mohammad Bavarian, Mark Chen, Heewoo Jun, Lukasz Kaiser, Matthias Plappert, Jerry Tworek, Jacob Hilton, Reiichiro Nakano, et al. Training verifiers to solve math word problems. [arXiv preprint arXiv:2110.14168](https://arxiv.org/abs/2110.14168), 2021.
- [12] CMeKG\_tools Contributors. Cmekg\_tools: Chinese medical knowledge graph tools. [https://github.com/king-yyf/CMeKG\\_tools](https://github.com/king-yyf/CMeKG_tools), 2023.
- [13] Weihao Cui, Yukang Chen, Han Zhao, Ziyi Xu, Quan Chen, Xusheng Chen, Yangjie Zhou, Shixuan Sun, and Minyi Guo. Optimizing slo-oriented llm serving with pd-multiplexing, 2025.

[14] Abhimanyu Dubey, Abhinav Jauhri, Abhinav Pandey, Abhishek Kadian, Ahmad Al-Dahle, Aiesha Letman, Akhil Mathur, Alan Schelten, Amy Yang, Angela Fan, Anirudh Goyal, Anthony Hartshorn, Aobo Yang, Archi Mitra, Archie Sravankumar, Artem Korenev, Arthur Hinsvark, Arun Rao, Aston Zhang, Aurélien Rodriguez, Austen Gregerson, Ava Spataru, Baptiste Rozière, Bethany Biron, Binh Tang, Bobbie Chern, Charlotte Caucheteux, Chaya Nayak, Chloe Bi, Chris Marra, Chris McConnell, Christian Keller, Christophe Touret, Chunyang Wu, Corinne Wong, Cristian Canton Ferrer, Cyrus Nikolaidis, Damien Allonsius, Daniel Song, Danielle Pintz, Danny Livshits, David Esiobu, Dhruv Choudhary, Dhruv Mahajan, Diego Garcia-Olano, Diego Perino, Dieuwke Hupkes, Egor Lakomkin, Ehab AlBadawy, Elina Lobanova, Emily Dinan, Eric Michael Smith, Filip Radenovic, Frank Zhang, Gabriel Synnaeve, Gabrielle Lee, Georgia Lewis Anderson, Graeme Nail, Grégoire Mialon, Guan Pang, Guillem Cucurell, Hailey Nguyen, Hannah Korevaar, Hu Xu, Hugo Touvron, Iliyan Zarov, Imanol Arrieta Ibarra, Isabel M. Kloumann, Ishan Misra, Ivan Evtimov, Jade Copet, Jaewon Lee, Jan Geffert, Jana Vranes, Jason Park, Jay Mahadeokar, Jeet Shah, Jelmer van der Linde, Jennifer Billock, Jenny Hong, Jenya Lee, Jeremy Fu, Jianfeng Chi, Jianyu Huang, Jiawen Liu, Jie Wang, Jiecao Yu, Joanna Bitton, Joe Spisak, Jongsoo Park, Joseph Rocca, Joshua Johnstun, Joshua Saxe, Junteng Jia, Kalyan Vasuden Alwala, Kartikeya Upasani, Kate Plawiak, Ke Li, Kenneth Heafield, Kevin Stone, and et al. The llama 3 herd of models. [CoRR](#), abs/2407.21783, 2024.

[15] Shihong Gao, Xin Zhang, Yanyan Shen, and Lei Chen. Apt-serve: Adaptive request scheduling on hybrid cache for scalable llm inference serving. [Proc. ACM Manag. Data](#), 3(3), June 2025.

[16] Jianfeng Gu, Puxuan Wang, Isaac Nunezand, Kai Huang, and Michael Gerndt. Has-gpu: Efficient hybrid auto-scaling with fine-grained gpu allocation for slo-aware serverless inferences, 2025.

[17] Cunchen Hu, Heyang Huang, Liangliang Xu, Xusheng Chen, Jiang Xu, Shuang Chen, Hao Feng, Chenxi Wang, Sa Wang, Yungang Bao, Ninghui Sun, and Yizhou Shan. Inference without interference: Disaggregate llm inference for mixed downstream workloads, 2024.

[18] Jinqi Huang, Yi Xiong, Xuebing Yu, Wenjie Huang, Entong Li, Li Zeng, and Xin Chen. Slo-aware scheduling for large language model inferences, 2025.

[19] Huawei Technologies Co., Ltd. Ascend community hardware documentation. <https://www.hiascend.com/en/document?tag=hardware>, 2025.

[20] Juyong Jiang, Fan Wang, Jiasi Shen, Sungju Kim, and Sunghun Kim. A survey on large language models for code generation. [arXiv preprint arXiv:2406.00515](#), 2024.

[21] Woosuk Kwon, Zhuohan Li, Siyuan Zhuang, Ying Sheng, Lianmin Zheng, Cody Hao Yu, Joseph E. Gonzalez, Hao Zhang, and Ion Stoica. Efficient memory management for large language model serving with pagedattention. In [Proceedings of the ACM SIGOPS 29th Symposium on Operating Systems Principles](#), 2023.

[22] Baolin Li, Yankai Jiang, Vijay Gadepally, and Devesh Tiwari. Llm inference serving: Survey of recent advances and opportunities. In [2024 IEEE High Performance Extreme Computing Conference \(HPEC\)](#), pages 1–8, 2024.

- [23] Ruihao Li, Shagnik Pal, Vineeth Narayan Pullu, Prasoon Sinha, Jeeho Ryoo, Lizy K. John, and Neeraja J. Yadwadkar. Mirage: Kv cache optimization through parameter remapping for multi-tenant llm serving, 2025.
- [24] Xiaoyao Liang. Ascend AI Processor Architecture and Programming: Principles and Applications of CANN. Elsevier, 2020.
- [25] Heng Liao, Jiajin Tu, Jing Xia, Hu Liu, Xiping Zhou, Honghui Yuan, and Yuxing Hu. Ascend: a scalable and unified architecture for ubiquitous deep neural network computing : Industry track paper. In 2021 IEEE International Symposium on High-Performance Computer Architecture (HPCA), pages 789–801, 2021.
- [26] Heng Liao, Jiajin Tu, Jing Xia, Hu Liu, Xiping Zhou, Honghui Yuan, and Yuxing Hu. Ascend: a scalable and unified architecture for ubiquitous deep neural network computing: Industry track paper. In 2021 IEEE International Symposium on High-Performance Computer Architecture (HPCA), pages 789–801. IEEE, 2021.
- [27] Heng Liao, Jiajin Tu, Jing Xia, and Xiping Zhou. Davinci: A scalable architecture for neural network computing. In 2019 IEEE Hot Chips 31 Symposium (HCS), pages 1–44. IEEE Computer Society, 2019.
- [28] Aixin Liu, Bei Feng, Bing Xue, Bingxuan Wang, Bochao Wu, Chengda Lu, Chenggang Zhao, Chengqi Deng, Chenyu Zhang, Chong Ruan, et al. Deepseek-v3 technical report. arXiv preprint arXiv:2412.19437, 2024.
- [29] Xupeng Miao, Chunan Shi, Jiangfei Duan, Xiaoli Xi, Dahua Lin, Bin Cui, and Zhi-hao Jia. Spotserve: Serving generative large language models on preemptible instances. In Proceedings of the 29th ACM International Conference on Architectural Support for Programming Languages and Operating Systems, Volume 2, ASPLOS '24, page 1112–1127, New York, NY, USA, 2024. Association for Computing Machinery.
- [30] Chengyi Nie, Rodrigo Fonseca, and Zhenhua Liu. Aladdin: Joint placement and scaling for slo-aware llm serving. arXiv preprint arXiv:2405.06856, 2024.
- [31] Pratyush Patel, Esha Choukse, Chaojie Zhang, Aashaka Shah, Íñigo Goiri, Saeed Maleki, and Ricardo Bianchini. Splitwise: Efficient generative llm inference using phase splitting. In 2024 ACM/IEEE 51st Annual International Symposium on Computer Architecture (ISCA), pages 118–132, 2024.
- [32] Archit Patke, Dhemath Reddy, Saurabh Jha, Haoran Qiu, Christian Pinto, Chandra Narayanaswami, Zbigniew Kalbarczyk, and Ravishankar Iyer. Queue management for slo-oriented large language model serving. In Proceedings of the 2024 ACM Symposium on Cloud Computing, SoCC '24, page 18–35, New York, NY, USA, 2024. Association for Computing Machinery.
- [33] Ruoyu Qin, Zheming Li, Weiran He, Mingxing Zhang, Yongwei Wu, Weimin Zheng, and Xinran Xu. Mooncake: A kvcache-centric disaggregated architecture for llm serving. arXiv preprint arXiv:2407.00079, 2024.

[34] Chaoyi Ruan, Yinhe Chen, Dongqi Tian, Yandong Shi, Yongji Wu, Jialin Li, and Cheng Li. Dynaserve: Unified and elastic execution for dynamic disaggregated llm serving, 2025.

[35] Ying Sheng, Shiyi Cao, Dacheng Li, Coleman Hooper, Nicholas Lee, Shuo Yang, Christopher Chou, Banghua Zhu, Lianmin Zheng, Kurt Keutzer, et al. S-lora: Serving thousands of concurrent lora adapters. [arXiv preprint arXiv:2311.03285](#), 2023.

[36] Ying Sheng, Lianmin Zheng, Binhang Yuan, Zhuohan Li, Max Ryabinin, Beidi Chen, Percy Liang, Christopher Ré, Ion Stoica, and Ce Zhang. Flexgen: High-throughput generative inference of large language models with a single gpu. In [International Conference on Machine Learning](#), pages 31094–31116. PMLR, 2023.

[37] Mohammad Shoeybi, Mostofa Patwary, Raul Puri, Patrick LeGresley, Jared Casper, and Bryan Catanzaro. Megatron-lm: Training multi-billion parameter language models using model parallelism. [arXiv preprint arXiv:1909.08053](#), 2019.

[38] Sudipta Saha Shubha, Haiying Shen, and Anand Iyer. USHER: Holistic interference avoidance for resource optimized ML inference. In [18th USENIX Symposium on Operating Systems Design and Implementation \(OSDI 24\)](#), pages 947–964, Santa Clara, CA, July 2024. USENIX Association.

[39] Biao Sun, Ziming Huang, Hanyu Zhao, Wencong Xiao, Xinyi Zhang, Yong Li, and Wei Lin. Llumnix: Dynamic scheduling for large language model serving. In [18th USENIX Symposium on Operating Systems Design and Implementation \(OSDI 24\)](#), pages 173–191, Santa Clara, CA, July 2024. USENIX Association.

[40] Yinghao Tang, Tingfeng Lan, Xiuqi Huang, Hui Lu, and Wei Chen. Scorpio: Serving the right requests at the right time for heterogeneous slos in llm inference, 2025.

[41] Gemma Team, Thomas Mesnard, Cassidy Hardin, Robert Dadashi, Surya Bhupatiraju, Shreya Pathak, Laurent Sifre, Morgane Rivière, Mihir Sanjay Kale, Juliette Love, et al. Gemma: Open models based on gemini research and technology. [arXiv preprint arXiv:2403.08295](#), 2024.

[42] Hugo Touvron, Thibaut Lavril, Gautier Izacard, Xavier Martinet, Marie-Anne Lachaux, Timothée Lacroix, Baptiste Rozière, Naman Goyal, Eric Hambro, Faisal Azhar, et al. Llama: Open and efficient foundation language models. [arXiv preprint arXiv:2302.13971](#), 2023.

[43] Dave Van Veen, Cara Van Uden, Louis Blankemeier, Jean-Benoit Delbrouck, Asad Aali, Christian Bluethgen, Anuj Pareek, Małgorzata Polacin, Eduardo Pontes Reis, Anna Seehofnerova, et al. Clinical text summarization: adapting large language models can outperform human experts. [Research Square](#), pages rs–3, 2023.

[44] vLLM Community. vllm ascend plugin. <https://github.com/vllm-project/vllm-ascend>, 2024. Accessed: 2025-06-05.

[45] Bingyang Wu, Shengyu Liu, Yinmin Zhong, Peng Sun, Xuanzhe Liu, and Xin Jin. Loongserve: Efficiently serving long-context large language models with elastic sequence parallelism. In [Proceedings of the ACM SIGOPS 30th Symposium on Operating Systems](#)

Principles, SOSP '24, page 640–654, New York, NY, USA, 2024. Association for Computing Machinery.

- [46] Jingfeng Wu, Yiyuan He, Minxian Xu, Xitong Gao, Kejiang Ye, and Chengzhong Xu. Unlock the potential of fine-grained llm serving via dynamic module scaling, 2025.
- [47] Yu Wu, Tongxuan Liu, Yuting Zeng, Siyu Wu, Jun Xiong, Xianzhe Dong, Hailong Yang, Ke Zhang, and Jing Li. Arrow: Adaptive scheduling mechanisms for disaggregated llm inference architecture, 2025.
- [48] Yunshu Wu, Hayate Iso, Pouya Pezeshkpour, Nikita Bhutani, and Estevam Hruschka. Less is more for long document summary evaluation by LLMs. arXiv preprint arXiv:2309.07382, 2023.
- [49] Jing Xia, Chuanning Cheng, Xiping Zhou, Yuxing Hu, and Peter Chun. Kunpeng 920: The first 7-nm chiplet-based 64-core arm soc for cloud services. IEEE Micro, 41(5):67–75, 2021.
- [50] An Yang, Baosong Yang, Beichen Zhang, Binyuan Hui, Bo Zheng, Bowen Yu, Chengyuan Li, Dayiheng Liu, Fei Huang, Haoran Wei, Huan Lin, Jian Yang, Jianhong Tu, Jianwei Zhang, Jianxin Yang, Jiaxi Yang, Jingren Zhou, Junyang Lin, Kai Dang, Keming Lu, Keqin Bao, Kexin Yang, Le Yu, Mei Li, Mingfeng Xue, Pei Zhang, Qin Zhu, Rui Men, Runji Lin, Tianhao Li, Tingyu Xia, Xingzhang Ren, Xuancheng Ren, Yang Fan, Yang Su, Yichang Zhang, Yu Wan, Yuqiong Liu, Zeyu Cui, Zhenru Zhang, and Zihan Qiu. Qwen2.5 technical report. arXiv preprint arXiv:2412.15115, 2024.
- [51] Dingyan Zhang, Haotian Wang, Yang Liu, Xingda Wei, Yizhou Shan, Rong Chen, and Haibo Chen. {BlitzScale}: Fast and live large model autoscaling with  $o(1)$  host caching. In 19th USENIX Symposium on Operating Systems Design and Implementation (OSDI 25), pages 275–293, 2025.
- [52] Wei Zhang, Zhiyu Wu, Yi Mu, Banruo Liu, Myungjin Lee, and Fan Lai. Tempo: Application-aware llm serving with mixed slo requirements, 2025.
- [53] Wei Zhang, Zhiyu Wu, Yi Mu, Banruo Liu, Myungjin Lee, and Fan Lai. Tempo: Application-aware llm serving with mixed slo requirements. arXiv preprint arXiv:2504.20068, 2025.
- [54] Justin Zhao, Timothy Wang, Wael Abid, Geoffrey Angus, Arnav Garg, Jeffery Kinnison, Piero Molino, Travis Addair, and Devvret Rishi. Lora land: 310 fine-tuned llms that rival gpt-4 — a technical report. <https://predibase.com/blog/lora-land-fine-tuned-open-source-llms-that-outperform-gpt-4>, 2024.
- [55] Lianmin Zheng, Wei-Lin Chiang, Ying Sheng, Siyuan Zhuang, Zhanghao Wu, Yonghao Zhuang, Zi Lin, Zhuohan Li, Dacheng Li, Eric P. Xing, Hao Zhang, Joseph E. Gonzalez, and Ion Stoica. Judging llm-as-a-judge with mt-bench and chatbot arena. arXiv preprint arXiv:2306.05685, 2023.
- [56] Victor Zhong, Caiming Xiong, and Richard Socher. Seq2sql: Generating structured queries from natural language using reinforcement learning. arXiv preprint arXiv:1709.00103, 2017.

- [57] Yinmin Zhong, Shengyu Liu, Junda Chen, Jianbo Hu, Yibo Zhu, Xuanzhe Liu, Xin Jin, and Hao Zhang. Distserve: disaggregating prefill and decoding for goodput-optimized large language model serving. In Proceedings of the 18th USENIX Conference on Operating Systems Design and Implementation, OSDI'24, USA, 2024. USENIX Association.
- [58] Yuhang Zhou, Zhibin Wang, Guyue Liu, Shipeng Li, Xi Lin, Zibo Wang, Yongzhong Wang, Fuchun Wei, Jingyi Zhang, Zhiheng Hu, et al. Squeezing operator performance potential for the ascend architecture. In Proceedings of the 30th ACM International Conference on Architectural Support for Programming Languages and Operating Systems, Volume 2, pages 1156–1171, 2025.
- [59] Kan Zhu, Haiyang Shi, Le Xu, Jiaxin Shan, Arvind Krishnamurthy, Baris Kasikci, and Liguang Xie. Polyserve: Efficient multi-slo serving at scale, 2025.
- [60] Pengfei Zuo, Huimin Lin, Junbo Deng, Nan Zou, Xingkun Yang, Yingyu Diao, Weifeng Gao, Ke Xu, Zhangyu Chen, Shirui Lu, Zhao Qiu, Peiyang Li, Xianyu Chang, Zhengzhong Yu, Fangzheng Miao, Jia Zheng, Ying Li, Yuan Feng, Bei Wang, Zaijian Zong, Mosong Zhou, Wenli Zhou, Houjiang Chen, Xingyu Liao, Yipeng Li, Wenxiao Zhang, Ping Zhu, Yinggang Wang, Chuanjie Xiao, Depeng Liang, Dong Cao, Juncheng Liu, Yongqiang Yang, Xiaolong Bai, Yi Li, Huaguo Xie, Huatao Wu, Zhibin Yu, Lv Chen, Hu Liu, Yujun Ding, Haipei Zhu, Jing Xia, Yi Xiong, Zhou Yu, and Heng Liao. Serving large language models on huawei cloudmatrix384, 2025.

## A. Latency Prediction

Here, we give further clarification on the latency prediction first introduced in Section 3. We first recap the latency predictor in DistServe [57]. It estimates execution times for both the prefill and decode phases and enables latency-aware scheduling and dispatching. Prefill time ( $E_p$ ) represents the duration to process the prompt and generate the first token, while decode time per token ( $E_d$ ) models the cost of generating each subsequent token. This predictor supports accurate latency estimation across diverse request sizes and batching configurations.

To enable informed scheduling and dispatching decisions that respect latency constraints, the system employs a latency predictor, inspired by [57], to estimate execution times for both the prefill and decode phases of request processing. The prefill time ( $E_p$ ) corresponds to the time required to process the input prompt and generate the first token. It is modeled as a quadratic function of the input lengths in the batch as denoted in Equation 1.

The decode time per token ( $E_d$ ), which models the time to generate each subsequent token during inference, is estimated using Equation 2.

To determine the coefficients  $(a, b, c, a', b', c')$ , we use a request profiler that monitors the execution of real requests and collects tuples of the form  $(\beta, l_i, t_p, t_d)$ . Here,  $t_p$  and  $t_d$  represent the actual processing prefill and decode times. The samples are used to fit the model parameters via least squares regression, minimizing the total squared relative error between predicted and actual latencies. This approach ensure accurate latency predictions across varying request sizes and batching configurations.

The coefficients of  $E_p$  and  $E_d$  in § A are obtained by profiling the execution of real requests. Profiling is performed using various batch sizes ( $\beta$ ): 1, 2, 4, 8, 16, 32, 64, 96, 128, 160, and 192; and input lengths ( $l_i$ ): 4, 8, 16, 32, 48, 64, 96, 128, 192, 256, 284, 512, 768, 1024, 1536, and 2020.

## B. Computing Token Limit (ntoken)

Here we give a more detailed explanation of computing the token limit to extend that in Section 5. We compute a token limit (ntoken), which determines the maximum number of tokens the worker can safely accept without violating any latency constraints. It is constrained by both the TTFT and the TPOT of a request. To ensure that the TTFT requirement is satisfied, the total time before the first token is produced must be less than or equal to the TTFT. This includes both the request’s prefill time and its waiting time in the queue.

In the worst-case scenario, where a request arrives immediately after a dispatch, the waiting time is equal to the *mature time* of the worker, which includes the prefill time ( $E_P$ ) and the time needed to decode a number of tokens.

The decoding time is calculated as the product of the number of tokens ( $M$ ) and the per-token decoding latency ( $E_d$ ). The number of tokens is chosen so that the prefill time  $E_P$  is effectively amortized by the overlap between prefill and decoding, characterized by the time-saving rate ( $TPOT - E_d$ ).

This leads to the following constraint:

$$\begin{aligned}
E_{pr} + \text{waiting\_time} &\leq \text{TTFT}_r \\
E_{pr} + (E_P + M \times E_d) &\leq \text{TTFT}_r \\
E_{pr} + \left( E_P + \frac{E_P}{\text{TPOT} - E_d} \times E_d \right) &\leq \text{TTFT}_r \\
E_P + \frac{E_P}{\text{TPOT} - E_d} \times E_d &\leq \text{TTFT}_r
\end{aligned} \tag{7}$$

Here:

- $E_{pr}$  is the estimated execution time for request  $r$ ,
- $E_P$  is the prefill time,
- $E_d$  is the decoding time per token,
- $\text{TPOT}$  is the TPOT for requests in the worker,
- $\text{TTFT}_r$  is the TTFT constraint for request  $r$ .

To simplify calculation formula, we omit the quadratic coefficient  $c$  from the  $E_P$  model, assuming its impact is relatively small compared to the linear term in typical workloads. Additionally, since we calculate  $n_{token}$  before dispatching (and not per-request), we omit  $E_{pr}$  from the formula.

$$\begin{aligned}
E_P \left( \frac{\text{TPOT}}{\text{TPOT} - E_d} \right) &\leq \text{TTFT}_r \\
\Rightarrow n_{token} &\leq \frac{\text{TTFT} \times \text{TPOT} - \text{TTFT} \times E_d - a \times \text{TPOT}}{b \times \text{TPOT}}
\end{aligned}$$

This constraint formulation ensures that requests can be served within their latency requirements, even in the worst-case dispatching scenario.